

Use of High Volumes of Fly Ash to Improve ECC Mechanical Properties and Material Greenness

by En-Hua Yang, Yingzi Yang, and Victor C. Li

This paper reports on the development of high-performance fiber-reinforced cementitious composites (HPFRCC), taking into account environmental sustainability considerations. Engineered cementitious composites (ECC), a unique member of HPFRCC featuring high tensile ductility with ultra-high volumes of fly ash (HVFA) replacement (up to 85% by weight) of cement, are proposed in this paper. While micromechanics is applied in many aspects of the material design process, emphasis of this study is placed on the effect of fly ash content on altering material microstructure and mechanical properties. Experimental results show that HVFA ECCs, while incorporating high volumes of recycled fly ash, can retain a long-term tensile ductility of approximately 2 to 3%. Significantly, both the crack width and free drying shrinkage are reduced with an increase of the fly ash amount, which may benefit the long-term durability of HVFA ECC structures. Micro-mechanics analysis indicates that the increase of fiber/matrix interface frictional bond in HVFA ECCs is responsible for the tight crack width. In addition, HVFA ECCs show a robustness improvement by achieving more saturated multiple cracking while reducing environmental impact through the use of industrial waste stream material instead of cement.

Keywords: engineered cementitious composites; high-volume fly ash; sustainability.

INTRODUCTION

Concrete is the most popular construction material, with more than 11.4 billion tons of concrete consumed annually worldwide.¹ It has been reported that 2.2 billion tons of cement was produced in the year 2005.² The requirement of cement increases with time and it was estimated that each ton of cement produced generates an equal amount of carbon dioxide.³ The production of cement is responsible for 5% of global greenhouse gas emission created by human activities.⁴ Therefore, incorporating sustainability concerns into the design of civil engineering materials is urgently needed.

High-performance fiber-reinforced cementitious composites (HPFRCC) can significantly contribute to enhancing the service life of civil infrastructure. Among them, engineered cementitious composites (ECC) is a noticeable representative with unique tensile properties. Unlike conventional tension softening concrete and fiber-reinforced concrete (FRC), ECC exhibits metal-like tensile strain-hardening behavior after matrix first cracking. Figure 1 shows the typical tensile stress-strain curve of ECC. The tensile ductility of ECC is several hundred times that of normal concrete and the fracture toughness of ECC is similar to that of aluminum alloy.⁵ Notably, ECC uses short, randomly distributed fibers with a moderate volume fraction (2% or less in general). With this relatively small amount of short fibers, self-consolidating ECC^{6,7} has been designed for use with regular construction equipment.⁸ The high performance, moderate fiber content combination is attained by micromechanics-based

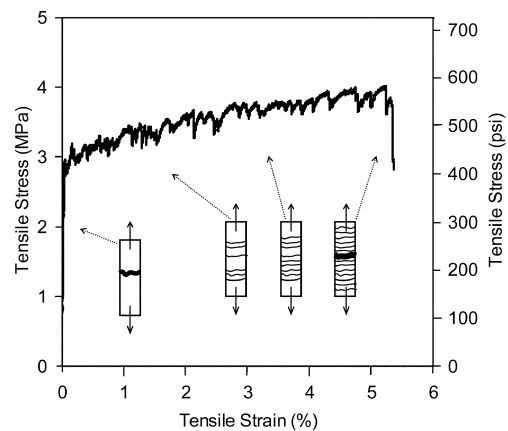


Fig. 1—Typical tensile stress-strain curve of ECC.

composite optimization.^{9,10} ECC is currently emerging in full-scale structural applications, including a composite ECC/steel deck of a cable-stayed bridge¹¹ and precast R/ECC coupling beams of several high-rise buildings¹¹ in Japan. In the U.S., a full-scale ECC bridge-deck link slab has been constructed in Michigan.¹² As broadening application of ECC materials is emerging, it is imperative to incorporate environmental concern into their development.

Compared with normal concrete, ECC uses more cement due to the absence of coarse aggregate in the mixture design. High cement content usually introduces higher hydration heat, autogenous shrinkage, and cost. Moreover, the associated increase in primary energy and emission of carbon dioxide create a negative environmental impact. A plausible solution would be to replace a large portion of cement in ECC by industrial by-product, for example, coal combustion products, without sacrificing its mechanical properties, in general, and tensile ductility, in particular.

Fly ash is a by-product of coal burning power plants and is usually considered a waste material. While more than 600 million tons of fly ash is generated each year worldwide, 80% is disposed of in landfills. With pozzolanic and cementitious properties, it has been used as a substitute for cement in concrete. Traditionally, the replacement of cement by fly ash is limited to approximately 10 to 25% of the total cementitious materials.^{13,14} With the progress in water-reducing chemical additives, high volume fly ash (HVFA) structural concrete

ACI Materials Journal, V. 104, No. 6, November-December 2007.

MS No. M-2006-340.R1 received January 31, 2007, and reviewed under Institute publication policies. Copyright © 2007, American Concrete Institute. All rights reserved, including the making of copies unless permission is obtained from the copyright proprietors. Pertinent discussion including authors' closure, if any, will be published in the September-October 2008 ACI Materials Journal if the discussion is received by June 1, 2008.

ACI member **En-Hua Yang** is a Graduate Student Research Assistant in the Department of Civil and Environmental Engineering at the University of Michigan, Ann Arbor, MI. He received his BS from National Cheng Kung University, Tainan, Taiwan; his MS from the National Taiwan University, Taipei, Taiwan; and his MSE from the University of Michigan. His research interests include the development and characterization of high-performance fiber-reinforced cementitious composites.

Yingzi Yang is an Associate Professor at the Harbin Institute of Technology (HIT), Harbin, China. She received her PhD from HIT. Her research interests include durability of concrete at sub-zero temperatures and durability of high-performance fiber-reinforced cementitious composites.

ACI member **Victor C. Li** is a Professor of civil and environmental engineering at the University of Michigan. He is a member of ACI Committee 544, Fiber Reinforced Concrete. His research interests include the micromechanics of cementitious materials; the design, characterization, and application of high ductility cement-based composites; and materials-based development of sustainable infrastructure.

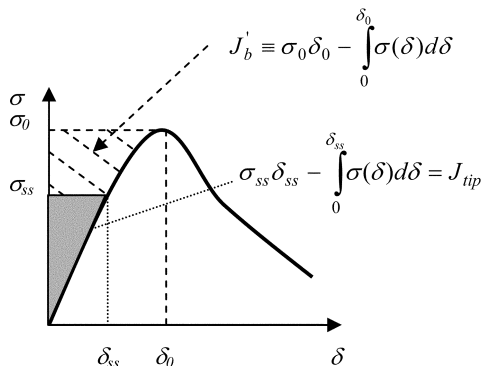


Fig. 2—Typical $\sigma(\delta)$ curve for tensile strain-hardening composite. Hatched area represents complementary energy J_b' . Shaded area represents crack tip toughness J_{tip} .

with reasonable compressive strength and workability was introduced.¹⁵ The term HVFA concrete is used to recognize a concrete material that has more fly ash than cement.¹⁴ It has been reported that concrete incorporating HVFA has significant improvement in mechanical properties and durability. Specifically, HVFA concrete has higher elastic modulus, lower shrinkage and creep, excellent freezing-and-thawing resistance, lower water permeability, and lower chloride-ion penetration.^{16,17} The practical use of HVFA concrete in full-scale structures was recently reported by Mehta.¹⁸

Previous research has developed green ECCs incorporating different types of fly ash, that is, bottom ash, Class F fly ash, and fine fly ash, with a fly ash-to-cement ratio (FA/C) up to 1.5.¹⁹ The cement content of green ECCs, however, is still twice that of normal concrete. This study focuses on incorporating a high dosage of Class F fly ash in ECC with an FA/C up to 5.6, in which the cement content is 40% less than normal concrete, and its resulting reduction in environmental impacts. The choice of Class F fly ash is due to its abundant availability (practical consideration) and less energy-intensity (that is, less post-processing) when compared with bottom ash and fine fly ash, respectively.

ECCs with ultra-high volume, low calcium fly ash replacement (up to 85% replacement by weight) are proposed. This paper focuses on the experimental characterization of mechanical properties and drying-shrinkage behavior of high volume Class F fly ash ECCs (HVFA ECC) and the effects of fly ash content in altering composite microstructures and environmental sustainability indicators. In the following sections, a brief review of ECC material design framework is introduced first. This design framework is

useful in HVFA ECC design and in understanding the experimental data on HVFA ECC tensile property characteristics. Experimental investigation is then described. HVFA ECC properties in terms of compressive strength, tensile stress-strain behavior, tensile ductility, crack width, robustness, and free drying shrinkage are reported. The microstructures of HVFA ECC are also investigated and related to composite macro behavior through micromechanics theory of ECC. Finally, material sustainability indicators (MSI) are reported.

RESEARCH SIGNIFICANCE

In the development of HPFRCC, material sustainability is seldom a concern and high cement content is commonly seen in the mixture design. In this study, a new set of ECC is developed taking into account environmental sustainability considerations. Specifically, a large amount of cement is substituted by recycled Class F fly ash. The resulting HVFA ECCs are expected to promote infrastructure sustainability through simultaneous enhancements of material greenness and infrastructure durability through tight crack width control.

ECC DESIGN THEORY

The strain-hardening behavior of ECC is a result of realizing and tailoring the synergistic interaction between fiber, matrix, and interface. Micromechanics has been used as a tool to link material microstructures to ECC composite properties. Desirable composite behavior can be tailored by control of material microstructures once the linkages are established.

ECC is a fiber-reinforced brittle mortar matrix composite and the pseudo strain-hardening behavior in ECC is achieved by sequential development of matrix multiple cracking (Fig. 1). The fundamental requirement for multiple cracking is that steady-state cracking prevails under tension, which requires the crack tip toughness J_{tip} to be less than the complementary energy J_b' calculated from the bridging stress σ versus crack opening δ curve, as illustrated in Fig. 2.^{20,21}

$$J_{tip} \leq \sigma_0 \delta_0 - \int_0^{\delta_0} \sigma(\delta) d\delta \equiv J_b' \quad (1)$$

$$J_{tip} = \frac{K_m^2}{E_m} \quad (2)$$

where σ_0 is the maximum bridging stress corresponding to the opening δ_0 , K_m is the matrix fracture toughness, and E_m is the matrix Young's modulus. Equation (1) employs the concept of energy balance during flat crack extension between external work, crack tip energy absorption through matrix breakdown (matrix toughness), and crack flank energy absorption through fiber/matrix interface debonding and sliding. This energy-based criterion determines the crack propagation mode (steady-state flat crack or Griffith crack).

The stress-crack opening relationship $\sigma(\delta)$, which can be viewed as the constitutive law of fiber bridging behavior, is derived by using analytic tools of fracture mechanics, micromechanics, and probabilistics. In particular, the energetics of tunnel crack propagation along fiber/matrix is used to quantify the debonding process and the bridging force of a fiber with a given embedment length.²² Probabilistics is introduced to describe the randomness of fiber location and orientation with respect to a crack plane. The random orientation of fiber

Table 1—Mixture proportion of HVFA ECCs

Mixture	FA/C	Cement, kg/m ³ (lb/yd ³)	Fly ash, kg/m ³ (lb/yd ³)	Sand, kg/m ³ (lb/yd ³)	Water, kg/m ³ (lb/yd ³)	High-range water-reducing admixture, kg/m ³ (lb/yd ³)	PVA fiber, kg/m ³ (lb/yd ³)	Total, kg/m ³ (lb/yd ³)
1	1.2	571 (962)	685 (1154)	456 (768)	332 (559)	6.80 (11.46)	26 (43.8)	2077 (3500)
2	1.6	477 (804)	763 (1286)	456 (768)	330 (556)	6.05 (10.19)	26 (43.8)	2060 (3471)
3	2.0	412 (694)	824 (1388)	456 (768)	326 (549)	5.52 (9.30)	26 (43.8)	2051 (3456)
4	2.4	362 (610)	870 (1466)	456 (768)	323 (544)	5.10 (8.59)	26 (43.8)	2042 (3441)
5	2.8	324 (546)	906 (1527)	456 (768)	320 (539)	5.29 (8.91)	26 (43.8)	2037 (3432)
6	3.2	292 (492)	935 (1575)	456 (768)	312 (526)	5.52 (9.30)	26 (43.8)	2027 (3415)
7	3.6	266 (448)	959 (1616)	456 (768)	309 (521)	5.80 (9.77)	26 (43.8)	2022 (3407)
8	5.6	190 (320)	1063 (1791)	456 (768)	300 (506)	6.45 (10.87)	26 (43.8)	2032 (3424)

also necessitates the accounting of the mechanics of interaction between an inclined fiber and the matrix crack. As a result, the $\sigma(\delta)$ curve is expressible as a function of micromechanics parameters, including interface chemical bond G_d , interface frictional bond τ_0 , and slip-hardening coefficient β accounting for the slip-hardening behavior during fiber pullout. In addition, snubbing coefficient f and strength reduction factor f' are introduced to account for the interaction between fiber and matrix as well as the reduction of fiber strength when pulled at an inclined angle. Besides interfacial properties, the $\sigma(\delta)$ curve is also governed by the matrix Young's modulus E_m , fiber content V_f , fiber diameter d_f , length L_f , and Young's modulus E_f .

Another condition for the pseudo strain-hardening is that the matrix tensile cracking strength σ_c must not exceed the maximum fiber bridging strength σ_0

$$\sigma_c < \sigma_0 \quad (3)$$

where σ_c is determined by the matrix fracture toughness K_m and preexisting internal flaw size a_0 . While the energy criterion (Eq. (1)) governs the crack propagation mode, the strength-based criterion represented by Eq. (3) controls the initiation of cracks. Satisfaction of both Eq. (1) and (3) is necessary to achieve ECC behavior; otherwise, normal tension-softening FRC behavior results. Details of these micromechanical analyses can be found in previous works.^{22,23}

Due to the random nature of preexisting flaw size and fiber distribution in ECC, a large margin between J_b' and J_{tip} is preferred. The pseudo strain-hardening (PSH) performance index has been used to quantitatively evaluate the margin and is defined as follows²⁴

$$PSH = \frac{J_b'}{J_{tip}} \quad (4)$$

Material with a larger PSH index should have a better chance of saturated multiple cracking. The saturation of multiple cracking is achieved when microcracks are more or less uniformly and closely spaced (at approximately 1 to 2 mm [0.039 to 0.078 in.]), and cannot be further reduced under additional tensile loading of a uniaxial tensile specimen. Robustness of tensile ductility refers to the consistency of tensile capacity from one specimen to another. To measure the extent of saturation of multiple cracking, PSH intensity has been used and is defined as crack spacing ratio²⁴

$$PSH \text{ Intensity} = \frac{x_d^{test}}{x_d} \quad (5)$$

Table 2—Physical properties and chemical compositions of fly ash

SiO ₂ , %	55.71	Moisture content, %	0.16
Al ₂ O ₃ , %	22.56	Loss on ignition, %	0.41
Fe ₂ O ₃ , %	5.61	Amount retained on No. 325 sieve, %	23.63
Sum, %	83.88	Specific gravity	2.29
CaO, %	10.44	Autoclave soundness, %	0.02
MgO, %	1.78	Strength activity index with portland cement at 7 days, % of control	77.1
SO ₃ , %	0.54		
Na ₂ O, %	0.24	Strength activity index with portland cement at 28 days, % of control	85.5
K ₂ O, %	0.79		
Total alkalis, %	0.76	Water required, % of control	94.6
Available alkalis, %	0.26		

where x_d is the theoretical crack spacing calculated from mechanics²⁵ and x_d^{test} is the crack spacing measured experimentally. Crack spacing herein is defined as the distance between two adjacent cracks. The minimum value of PSH intensity is 1, which indicates a fully saturated multiple cracking state. According to Aveston et al.,²⁶ the PSH intensity should fall between 1 and 2 for saturated PSH behavior.

The micromechanics-based strain-hardening criteria, Eq. (1) and (3), will be used as guidance for HVFA ECC design and in understanding the experimental data on HVFA ECC tensile property characteristics. The evaluation of PSH and PSH intensity is helpful in quantifying the saturation of multiple cracking and the robustness of tensile ductility for the newly developed HVFA ECCs.

EXPERIMENTAL INVESTIGATION

Materials

Previous research¹⁹ incorporating fly ash into ECC design ($FA/C = 0$ to 1.5) indicates that the use of fly ash reduces matrix toughness and fiber/matrix interfacial chemical bond, which makes the satisfaction of Eq. (1) easier to attain, and is therefore beneficial for ECC strain-hardening behavior. The use of higher fly ash content should make this effect more profound, and therefore eight HVFA ECCs with various fly ash contents (FA/C ranges from 1.2 to 5.6 by weight) were examined in this research. The mixture design of HVFA ECCs can be found in Table 1. Type I ordinary portland cement (OPC) was used in all mixtures. The fly ash used was an ASTM Class F fly ash from Texas and the physical properties and chemical compositions of the fly ash are listed in Table 2. A fine silica sand with a maximum grain size of 250 μm (0.01 in.) and a mean size of 110 μm (0.004 in.) was adopted in ECC mixtures. The size distribution of this quartz sand is listed in Table 3. In all mixtures, the water-cement ratio (w/c) was controlled at 0.25 ± 0.01 . Slight adjustment

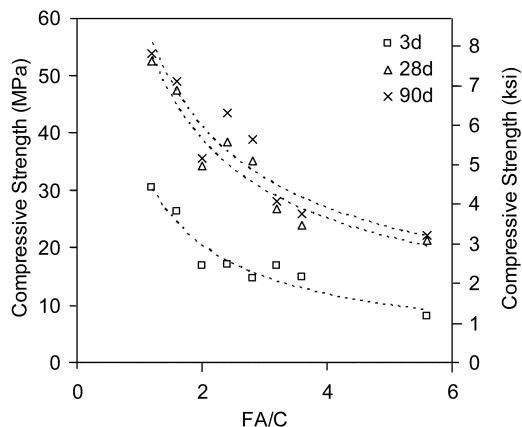


Fig. 3—Compressive strength of HVFA ECC as function of fly ash content at different ages.

Table 3—Size distribution of silica sand

< 150 μm (0.0059 in.), %	< 100 μm (0.0039 in.), %	< 75 μm (0.0030 in.), %	< 53 μm (0.0021 in.), %
93	77	33	8

in the amount of high-range water-reducing admixture and w/c in each mixture was performed to achieve consistent rheological properties for better fiber distribution and workability. All HVFA ECCs, therefore, have similar fresh properties with self-consolidating performance. While various fiber types have been used in the past, a polyvinyl alcohol (PVA) fiber was used at a moderate volume fraction of 2% in this study. The dimensions of the PVA fiber are 8 mm (0.315 in.) in length and 39 μm (0.0015 in.) in diameter on average. The nominal tensile strength of the fiber is 1600 MPa (11 psi) and the density of the fiber is 1300 kg/m^3 (2192 lb/yd^3). The fiber is surface-coated by oil (1.2% by weight) to reduce the fiber/matrix interfacial bond strength. This decision was made through ECC micromechanics material design theory and has been experimentally demonstrated from previous investigations.^{27,28}

Mixing and curing

A mixer with 13 L (0.46 ft^3) capacity was used in preparing all ECC mixtures. Solid ingredients, including cement, fly ash, and sand, were first mixed for a couple of minutes. Water and high-range water-reducing admixture were then added into the dry mixture and mixed for another 3 minutes. The liquefied fresh mortar matrix should reach a consistent and uniform state before adding fibers. After examining the mortar matrix and making sure there is no clump in the bottom of the mixer, PVA fibers were slowly added into the mortar matrix and mixed until all fibers are evenly distributed. The mixture was then cast into molds. Specimens were demolded after 24 hours. After demolding, specimens were first cured in sealed bags at room temperature (20 °C [68 °F]) for 7 days and then cured in air at room temperature before testing. The RH of the laboratory air was 45% \pm 5%.

Specimens

A compressive test was carried out for each mixture at the age of 3, 28, and 90 days. Cylinders measuring 75 mm (3 in.) in diameter and 150 mm (6 in.) in length were used in this study. The ends of cylinders were capped with a sulfur

compound to ensure a flat and parallel surface and a better contact with the loading device.

Coupon specimens measuring 152 x 76 x 13 mm (6 x 3 x 0.5 in.) were used to conduct uniaxial tensile test for each mixture at the age of 3, 28, and 90 days. Uniaxial tensile tests give material tensile stress-strain behavior. In addition, crack width, another important tensile characterization of ECC material in relation to durability,^{29,30} was also examined. A servohydraulic testing system was used in displacement control mode to conduct the tensile test. The loading rate used was 0.0025 mm/second (0.0001 in./second) to simulate a quasi-static loading condition. Aluminum plates were glued on both sides at the ends of the coupon specimens to facilitate gripping. Two external linear variable displacement transducers were attached to the specimen with a gauge length of approximately 50 mm (2 in.) to measure the specimen deformation.

The matrix fracture toughness K_m at the age of 28 days was measured by the three-point bending test according to ASTM E 399. Beam specimens measuring 305 mm (12 in.) in length, 76 mm (3 in.) in height, and 38 mm (1.5 in.) in thickness were cast from selected mixtures (Mixtures 1, 2, 3, 5, and 7) without adding fibers. The span of support is 254 mm (10 in.) and the notch depth to height ratio is 0.5.

A single-fiber pullout test was performed for Mixtures 1, 2, 3, 5, and 7 at the age of 28 days to quantify fiber/matrix interfacial properties as a function of fly ash content. Three important interfacial parameters, including chemical bond strength G_d , frictional bond strength τ_0 , and slip hardening coefficient β , were determined through this test. Specimen preparation, test configuration, data processing, and calculation of interfacial parameters can be found in Reference 31. The interfacial parameters along with other micromechanics parameters were then used to calculate the fiber bridging law $\sigma(\delta)$.²² The resulting complementary energy J_b' calculated from the $\sigma(\delta)$ curve combined with the matrix fracture toughness J_{tip} obtained from the K_m measurement were used as inputs to evaluate material behavior, that is, strain-hardening or tension softening, and to calculate the PSH index.

Free drying shrinkage measurements were made for all eight HVFA ECCs as a function of drying time. Tests were conducted according to ASTM C 157/C 157M and ASTM C 596 standards, except that the storing of the specimens before the test was modified. The specimens were cured in sealed bags for 7 days before they were moved to laboratory air and the measurement was started. Free drying shrinkage deformation was monitored until hygral equilibrium was reached.

EXPERIMENTAL RESULTS AND DISCUSSION

The compressive strength of eight HVFA ECCs with different fly ash contents at the ages of 3, 28, and 90 days is summarized in Fig. 3 and Table 4. Each data point is an average of at least three compressive tests. As can be seen from the curve, the replacement of cement by Class F fly ash generally reduces the compressive strength of ECC at all ages. Even at 75% replacement of cement ($FA/C = 2.8$), however, the compressive strength of ECC at 28 days can still reach 35 MPa (5075 psi), which exceeds the nominal compressive strength for normal concrete (30 MPa [4350 psi]). No significant strength gain is found in HVFA ECCs between 28 to 90 days. Fly ash is usually considered a beneficial ingredient for long-term strength development in concrete due to its pozzolanic properties. In HVFA ECC, however, secondary hydration of fly ash may only reach a very limited reaction degree because the fly ash content is relatively high

Table 4—Compressive strength, MPa (ksi) of HVFA ECCs at different ages

FA/C age, days	1.2	1.6	2.0	2.4	2.8	3.2	3.6	5.6
3	30.6 ± 2.1 (4.4 ± 0.3)	26.3 ± 1.0 (3.8 ± 0.2)	16.9 ± 0.4 (2.4 ± 0.1)	17.1 ± 0.4 (2.5 ± 0.1)	14.6 ± 3.2 (2.1 ± 0.5)	17.0 ± 0.5 (2.5 ± 0.1)	15.0 ± 0.2 (2.2 ± 0.0)	8.2 ± 0.2 (1.2 ± 0.0)
28	52.6 ± 0.2 (7.6 ± 0.0)	47.5 ± 0.4 (6.9 ± 0.1)	34.2 ± 2.8 (5.0 ± 0.2)	38.4 ± 1.6 (5.6 ± 0.2)	35.2 ± 1.3 (5.1 ± 0.2)	26.7 ± 4.4 (3.9 ± 0.6)	23.9 ± 1.0 (3.5 ± 0.1)	21.4 ± 1.0 (3.1 ± 0.1)
90	54.0 ± 1.4 (7.8 ± 0.2)	49.0 ± 4.8 (7.1 ± 0.7)	35.5 ± 2.9 (5.2 ± 0.1)	43.4 ± 0.6 (6.3 ± 0.1)	38.9 ± 1.1 (5.6 ± 0.2)	28.2 ± 1.2 (4.1 ± 0.2)	25.9 ± 0.1 (3.8 ± 0.0)	22.2 ± 1.4 (3.2 ± 0.2)

Table 5—Tensile strain capacity (percent) of HVFA ECCs at different ages

FA/C age, days	1.2	1.6	2.0	2.4	2.8	3.2	3.6	5.6
3	4.6 ± 1.3	4.2 ± 0.8	4.1 ± 0.2	4.3 ± 1.0	4.4 ± 0.3	4.3 ± 1.1	4.0 ± 0.3	3.8 ± 0.4
28	2.7 ± 1.1	3.7 ± 0.6	3.0 ± 1.1	2.9 ± 0.8	3.0 ± 0.7	2.7 ± 0.7	2.5 ± 0.3	3.3 ± 0.2
90	1.8 ± 0.9	3.0 ± 1.4	3.1 ± 1.5	2.3 ± 0.7	3.3 ± 1.4	2.9 ± 0.9	2.6 ± 1.2	3.4 ± 0.6

Table 6—Residual crack width (µm) after tensile test of HVFA ECCs at different ages

FA/C age, days	1.2	1.6	2.0	2.4	2.8	3.2	3.6	5.6
3	84 ± 32	60 ± 7	33 ± 6	28 ± 6	16 ± 4	13 ± 5	12 ± 2.5	13 ± 2
28	31 ± 6	36 ± 12	15 ± 3	22 ± 6	15 ± 8	8 ± 2	8 ± 1	15 ± 2
90	17 ± 5	26 ± 10	16 ± 6	16 ± 8	11 ± 3	8 ± 2	7 ± 1	9 ± 1

in proportion to cement and fly ash may remain in the system as fillers even after a long time of curing. The second reason is that the very low water-cementitious material ratio (*w/cm*) provides limited water to promote the reaction of secondary hydration between fly ash and cement products. The third possible reason is that specimens were cured in air after 7 days sealed curing. Related research indicated that hydration of cement will stop completely when the internal humidity in hardened cement paste falls below 80%.³² Therefore, loss of internal humidity in low *w/cm* HVFA ECCs may arrest further hydration.

Figure 4 shows the representative 28-day tensile stress-strain curves of HVFA ECCs. Tensile ductility at different ages is summarized in Table 5 and is plotted against *FA/C* illustrated in Fig. 5. Each data point in Fig. 5 is an average of four or more uniaxial tensile tests. From the uniaxial tensile test, all HVFA ECCs exhibit tensile strain hardening behavior at different ages and the tensile strain capacity reaches 2 to 3% at the age of 90 days. This indicates that the most unique property of ECC, tensile ductility, is retained and is not sacrificed by replacing cement with a large amount of Class F fly ash.

The crack width of ECC at the material hardening stage does not depend on structural geometry and has been recognized as an important material property.³³ The imposed deformation is accommodated by ECC multiple cracks with constant crack width during the strain-hardening stage, as shown in Fig. 1. The magnitude of the crack width controls many transport properties in cracked concrete materials and has a direct impact on durability.^{29,30} Table 6 and Fig. 6 give the effect of fly ash content on the residual crack width at different ages. The term residual crack width indicates that the crack width is measured from the unloaded specimen after the uniaxial tensile test. It was observed in this study that the width of a loaded crack is approximately two times the width of the unloaded one. Each data point in Fig. 6 is an average of four or more coupon specimens and 20+ crack widths are measured from each specimen. It was found that the crack width reduces as fly ash content increases at all ages. The drop is significant, especially in early ages (3 days, Fig. 7). At the age of 28 days, the residual crack width of

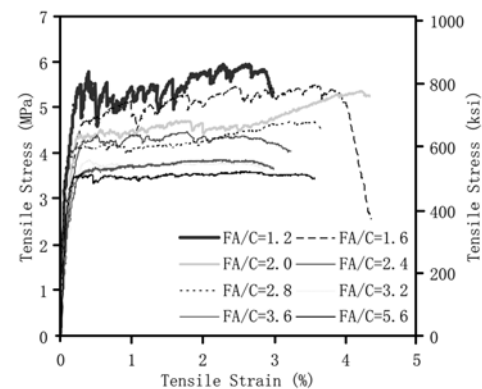


Fig. 4—Tensile stress-strain curve of HVFA ECCs at age of 28 days.

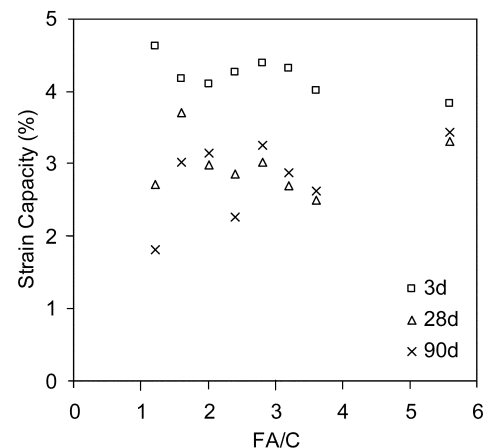


Fig. 5—Tensile ductility of HVFA ECC as function of fly ash content at different ages.

some HVFA ECCs can be lower than 10 µm (0.0004 in.). This observation suggests that HVFA ECC will most likely have lower permeability and better durability even in the presence of microcracks when compared with cracked concrete

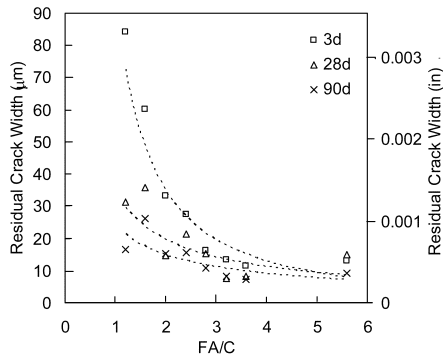


Fig. 6—Residual crack width of HVFA ECC as function of fly ash content at different ages.

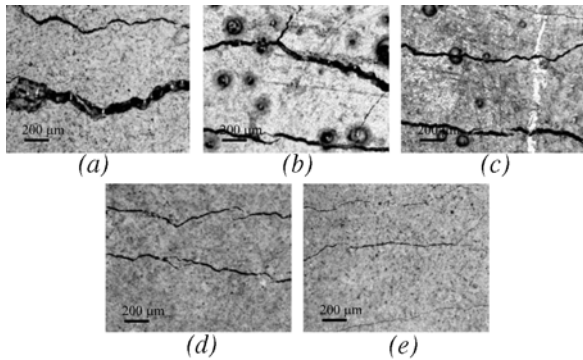


Fig. 7—Microscopic photos of residual crack width of HVFA ECCs at age of 3 days where FA/C are: (a) 1.2; (b) 1.6; (c) 2.0; (d) 2.8; and (e) 3.6, respectively.

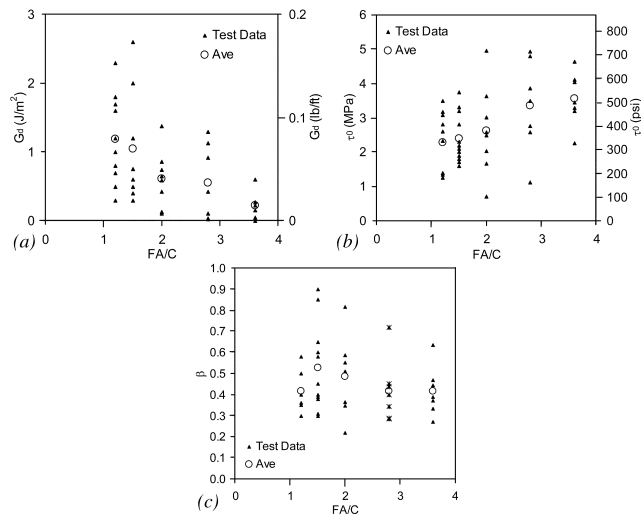


Fig. 8—(a) Chemical bond strength; (b) frictional bond strength; and (c) slip-hardening coefficient of HVFA ECC as function of fly ash content at age of 28 days.

in which the crack width is not self-controlled and is usually in the range of several hundred micron meters to several millimeters. In addition, the crack width was identified as a key factor in the self-healing of ECC.³⁴ Tight crack widths in HVFA ECC are likely to promote self-healing behavior.

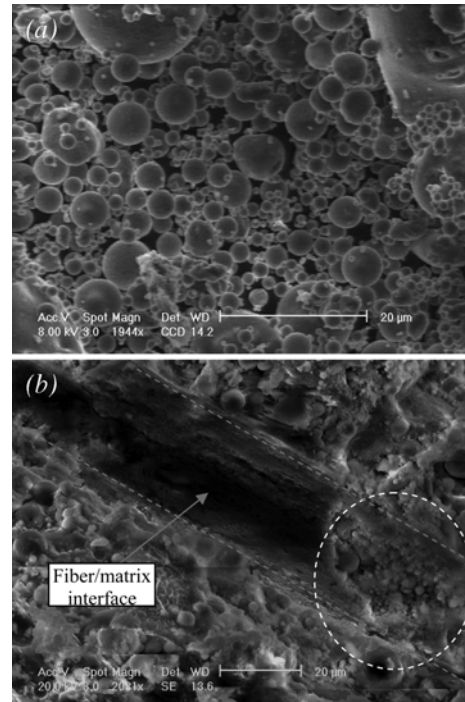


Fig. 9—SEM photos of: (a) Class F fly ash; and (b) ITZ of HVFA ECC with 85% replacement of cement at age of 90 days.

A single fiber pullout test was carried out to reveal the effect of fly ash content on fiber/matrix interfacial properties and on crack width control of HVFA ECCs. Single fiber pullout specimens were cast from selected mixtures (Mixtures 1, 2, 3, 5, and 7) and tested after curing for 28 days. Results are presented in Fig. 8. As can be seen, the chemical bond G_d drops with an increase of fly ash content. Lower G_d indicates easier interface debonding without fiber breaking. This is a result of lower hydration degree in fiber/matrix interface as more cement is replaced by fly ash. The chemical bond of PVA fiber to cementitious matrix is believed to be governed by the formation of a metal hydroxide layer in the interfacial transition zone (ITZ), in particular calcium hydroxide.³⁵ In fact, build-up of $\text{Ca}(\text{OH})_2$ crystals at the PVA fiber surface was observed.^{35,36} In the composition of fly ash, most Ca^{2+} ions are not free. Hence, the high volume fraction of low calcium Class F fly ash serves as an inner filler, dilutes the concentration of Ca^{2+} in the matrix, and reduces the possibility of developing a strong chemical bond.

Interestingly, the frictional bond τ_0 shows a reverse trend. High τ_0 indicates a strong holding force in the interface and resistance to fiber sliding. As a result, crack width reduction is attained at higher fly ash content. A possible mechanism that contributes to higher τ_0 may be that unhydrated fly ash with smooth spherical shape (Fig. 9(a)) and small particle size ($76.37\% < 45 \mu\text{m}$ [0.0018 in.]) increases the compactness of ITZ,³⁷ and therefore increases interface frictional bond. Figure 9(b) illustrates the densely packed fiber/matrix interface in HVFA ECC. This picture was taken from a HVFA ECC with 85% replacement of cement ($\text{FA/C} = 5.6$) by a scanning electron microscope (SEM) at an age of 90 days. The dark groove shows the impression left by a fiber (removed before taking this image) on the fiber/matrix interface (marked by the dash line). The circled area shows the morphology right beneath the fiber/matrix interface. To a certain degree, it reflects the structure of ITZ. It is clear that many unhydrated fly

ash particles serving as inner fillers are distributed in the matrix and densely pack the interface zone. The slip-hardening coefficient was found to be independent of fly ash content as shown in Fig. 8(c).

Figure 10 gives the result of the PSH index of HVFA ECCs as a function of fly ash contents at the age of 28 days. To calculate the PSH index, the complementary energy J_b' was read out from the $\sigma(\delta)$ curve, which was calculated from the measured interfacial properties through micromechanics models²² and the matrix toughness J_{tip} is determined by Eq. (2) using experimentally measured matrix fracture toughness K_m and the matrix Young's modulus. As can be seen, HVFA ECCs have PSH indexes larger than one, which means the satisfaction of Eq. (1), consistent with the observation that all HVFA ECCs exhibited tensile strain-hardening behavior. Moreover, ECC with higher fly ash content has higher value of PSH index, which indicates a larger margin between J_b' and J_{tip} and implies a better chance of saturated multiple cracking, that is, a more robust multiple cracking behavior in HVFA ECCs.

This implication was further confirmed by plotting the inverse of PSH intensity index, $(PSH \text{ intensity})^{-1}$, against FA/C as depicted in Fig. 10. The PSH intensity index was evaluated based on the observed crack spacing x_d^{test} measured from the uniaxial tensile tests and the theoretical crack spacing x_d calculated from the mechanics of matrix stress build-up through interfacial shear stress transfer. Detailed calculation of x_d can be found in Reference 25. The maximum value of $(PSH \text{ intensity})^{-1}$ is 1, which indicates a fully saturated multiple cracking. A larger $(PSH \text{ intensity})^{-1}$ value represents more saturate and robust multiple cracking behavior (that is, robust tensile strain capacity). Indeed, the PSH index is positively correlated with $(PSH \text{ intensity})^{-1}$, as shown in Fig. 10, and therefore the PSH index can be used as an indicator in the future to identify the saturation of multiple cracking and the robustness of ECC tensile ductility. Robustness improvement of HVFA ECC in terms of tensile strain capacity is evident due to easy saturation of multiple cracking and is almost linearly proportional to the fly ash content, as illustrated in Fig. 10.

Figure 11 shows the free drying shrinkage deformation measurement of HVFA ECCs. Because of the absence of coarse aggregate, drying shrinkage deformation of ECC ($FA/C = 1.2$, the far left point in Fig. 11) is higher than normal structural concrete.³⁸ The general trend in Fig. 11 shows that fly ash can effectively reduce free drying shrinkage deformation in ECC material. Similar results have been reported for HVFA concrete.³⁹ In the present study, a 50% reduction of free drying shrinkage of ECC was found when the FA/C was increased from 1.2 to 5.6. A possible mechanism contributing to the reduction of free drying shrinkage in HVFA ECCs is matrix densification, which may prevent internal moisture evaporation. Matrix densification in fly ash concrete has been extensively documented in the literature.⁴⁰ This is typically attributed to the shape, pozzolanic property, and micro-filler effect of fly ash. An alternative mechanism is that unhydrated fly ash particles serve as fine aggregates (Fig. 9(b)) to restrain the shrinkage deformation.^{14,41}

To quantify the greenness of HVFA ECCs, MSI are adopted in this study.⁴² MSIs are calculated based on material and energy flow in the production process, and expressed in terms of energy consumption, waste, and pollutant releases including solid waste, carbon dioxide, nitrogen oxides, sulfur oxides, particulate matter, water usage, hydrocarbon demand,

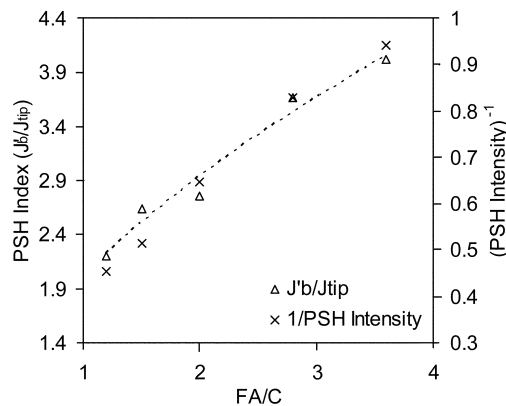


Fig. 10—PSH and PSH intensity indexes of HVFA ECCs at age of 28 days.

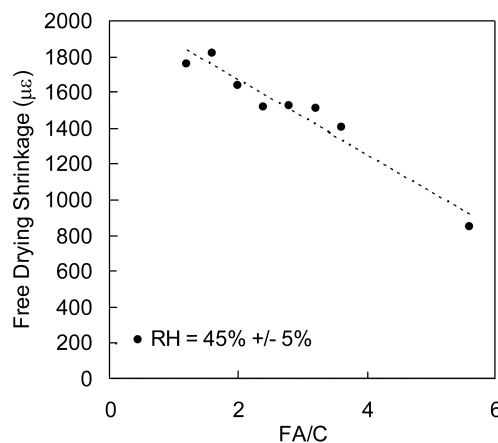


Fig. 11—Free drying shrinkage of HVFA ECC as function of fly ash content.

Table 7—Material sustainable indicators of conventional concrete and HVFA ECCs

	Total energy, MJ/L (MJ/gal.)	Solid waste, kg/L (lb/gal.)	Carbon dioxide, g/L (lb/gal.)
Conventional concrete	2.46 (9.32)	0.2 (1.669)	373.28 (3.12)
HVFA ECC (FA/C = 1.2)	5.99 (22.69)	-0.46 (-3.84)	628.16 (5.24)
HVFA ECC (FA/C = 3.6)	4.35 (16.48)	-0.84 (-7.01)	350.79 (2.93)
HVFA ECC (FA/C = 5.6)	3.91 (14.81)	-0.95 (-7.93)	276.95 (2.31)

and others. Four assumptions are made in calculating the contribution of fly ash to MSI. First, fly ash is a waste material that would be disposed of. Second, fly ash does not carry any environmental burdens associated with coal combustion. Third, reusing fly ash is given a credit for saving landfill space. Fourth, there is no processing on fly ash after leaving the power plant. Table 7 summarizes three major MSIs of representative HVFA ECCs. MSIs of conventional concrete are also computed for the comparison purpose. In calculating solid waste, fly ash is assigned a negative value because the recycling removes fly ash from global waste flow. In general, MSIs decrease with an increase of FA/C , which indicates a greener material at higher fly ash content. Due to

the presence of fiber, HVFA ECCs consume more energy than concrete. In the production of solid waste and carbon dioxide, however, the material sustainability performance of HVFA ECCs has surpassed conventional concrete. Although MSIs provide a simple platform for comparing greenness of different materials, true assessment of sustainability should be performed based on life-cycle analysis of a specific type of infrastructure.⁴³

CONCLUSIONS

A set of HVFA ECCs with different amounts of fly ash replacement was developed. This study demonstrates the feasibility of creating greener ECC, which maintains the tensile ductility characteristics but also incorporates sustainability considerations. In particular, the following conclusions can be drawn:

1. An increase of fly ash content generally reduces the compressive strength of ECC. At FA/C equals 2.8, however, the compressive strength at 28 days can still reach 35 MPa, which is the regular strength grade for concrete in many applications. HVFA ECCs with different compressive strength may be selected for use in different applications;

2. All HVFA ECCs show tensile strain-hardening behavior, with PSH indexes larger than one. At the age of 90 days, the tensile ductility of HVFA ECCs can still reach the long-term stabilized value of 2 to 3%;

3. High fly ash content tends to reduce the crack width in ECC. It is found that high interface frictional bond τ_0 restrains the slippage of fiber and is responsible for the tight crack width. Microstructure analysis reveals that high τ_0 is a result of densely packed interface transition zone by unhydrated fly ash particles. Tight crack widths have been shown to promote self-healing in ECC and greatly benefit the durability of ECC infrastructure;

4. Increasing the amount of fly ash in HVFA ECCs tends to improve robustness (reduced variability) of tensile ductility based on the current analysis. Furthermore, the PSH index may be used as a robustness indicator in terms of ECC tensile ductility;

5. Incorporating high volumes of fly ash in ECC generally reduces the free drying shrinkage. It may be a result of matrix densification and/or unhydrated fly ash constraint effect. In this study, 50% reduction of free drying shrinkage is found when FA/C increases from 1.2 to 5.6;

6. In MSI analysis, HVFA ECCs remain more energy intensive than conventional concrete. The production of HVFA ECCs, however, results in negative solid waste and in some cases lower carbon dioxide emission compare with that of conventional concrete; and

7. Incorporating waste stream material ingredients does not necessarily mean lower composite material performance, as long as the governing mechanisms for possible deterioration are controlled. In the present study, using recycled Class F fly ash actually improves many properties of ECC, especially reduced drying shrinkage, tighter crack width, and more robust tensile strain ductility. Therefore, understanding the underlying micromechanics of critical composite properties is the key to successfully take sustainability into consideration in the design of civil engineering materials.

ACKNOWLEDGMENTS

This research was funded through an NSF MUSES Biocomplexity Program Grant (CMS-0223971 and CMS-0329416). MUSES (Materials Use: Science, Engineering, and Society) supports projects that study the reduction of adverse

human impact on the total interactive system of resource use, the design and synthesis of new materials with environmentally benign impacts on biocomplex systems, as well as the maximization of efficient use of materials throughout their life cycles. The authors would like to acknowledge helpful input from M. Lepech and G. Keoleian, especially on the computation of the material sustainability indexes.

REFERENCES

1. Metha, P. K., "Reducing the Environmental Impact of Concrete," *Concrete International*, V. 23, No. 10, Oct. 2001, pp. 61-66.
2. USGS, *Mineral Commodity Summaries*, 2006.
3. van Oss, H. G., and Padovani, A. C., "Cement Manufacture and the Environment—Part I: Chemistry and Technology," *Journal of Industrial Ecology*, V. 6, No. 1, 2002, pp. 89-105.
4. Battelle, "Climate Change," *Toward a Sustainable Cement Industry*, World Business Council on Sustainable Development (WBCSD), 2002.
5. Maalej, M.; Hashida, T.; and Li, V. C., "Effect of Fiber Volume Fraction on the Off-Crack Plane Energy in Strain-Hardening Engineered Cementitious Composites," *Journal of the American Ceramics Society*, V. 78, No. 12, 1995, pp. 3369-3375.
6. Kong, H. J.; Bike, S.; and Li, V. C., "Development of a Self-Consolidating Engineered Cementitious Composite Employing Electrosteric Dispersion/Stabilization," *Journal of Cement and Concrete Composites*, V. 25, No. 3, 2003, pp. 301-309.
7. Kong, H. J.; Bike, S.; and Li, V. C., "Constitutive Rheological Control to Develop a Self-Consolidating Engineered Cementitious Composite Reinforced with Hydrophilic Poly(vinyl alcohol) Fibers," *Journal of Cement and Concrete Composites*, V. 25, No. 3, 2003, pp. 333-341.
8. Li, V. C.; Lepech, M.; and Li, M., "Field Demonstration of Durable Link Slabs for Jointless Bridge Decks Based on Strain-Hardening Cementitious Composites," *Michigan DOT Report*, 2005.
9. Li, V. C., "Engineered Cementitious Composites—Tailored Composites Through Micromechanical Modeling," *Fiber Reinforced Concrete: Present and the Future*, N. Banthia, A. Bentur, and A. Mufit, eds., Canadian Society for Civil Engineering, Montreal, QC, Canada, 1997, pp. 64-97.
10. Lin, Z., and Li, V. C., "Crack Bridging in Fiber Reinforced Cementitious Composites with Slip-Hardening Interface," *Journal of Mechanics and Physics of Solids*, V. 45, No. 5, 1997, pp. 763-787.
11. Kunieda, M., and Rokugo, K., "Recent Progress on HPRCC in Japan," *Journal of Advanced Concrete Technology*, V. 4, No. 1, 2006, pp. 19-33.
12. Michigan DOT, "Bridge Decks Going Jointless: Cementitious Composites Improve Durability of Link Slabs," *Construction and Technology Research Record*, V. 100, 2005, pp. 1-4.
13. Reiner, M., and Rens, K., "High-Volume Fly Ash Concrete: Analysis and Application," *Practice Periodical on Structural Design and Construction*, V. 11, No. 1, 2006, pp. 58-64.
14. Zhang, M. N., "Microstructure, Crack Propagation, and Mechanical Properties of Cement Pastes Containing High Volumes of Fly Ashes," *Cement and Concrete Research*, V. 25, No. 6, 1995, pp. 1165-1178.
15. Malhotra, V. M., "Superplasticized Fly Ash Concrete for Structural Concrete Applications," *Concrete International*, V. 8, No. 12, Dec. 1986, pp. 28-31.
16. Sivasundaram, V.; Crette, G. G.; and Malhotra, V. M., "Mechanical Properties, Creep, and Resistance to Diffusion of Chloride Ions of Concretes Incorporating High Volumes of ASTM Class F Fly Ashes from Seven Different Sources," *ACI Materials Journal*, V. 88, No. 4, July-Aug. 1991, pp. 407-416.
17. Bilodeau, A.; Sivasundaram, V.; Painter, K. E.; and Malhotra, V. M., "Durability of Concrete Incorporating High Volumes of Fly Ash from Sources in the U.S.A.," *ACI Materials Journal*, V. 91, No. 1, Jan.-Feb. 1994, pp. 3-12.
18. Mehta, P. K., and Manmohan, D., "Sustainable High-Performance Concrete Structures," *Concrete International*, V. 28, No. 7, July 2006, pp. 37-42.
19. Wang, S., "Micromechanics Based Matrix Design for Engineered Cementitious Composites," Department of Civil and Environmental Engineering, University of Michigan, Ann Arbor, MI, 2005.
20. Marshall, D. B., and Cox, B. N., "A J-Integral Method for Calculating Steady-State Matrix Cracking Stresses in Composites," *Mechanics of Materials*, V. 8, 1988, pp. 127-133.
21. Li, V. C., and Leung, C. K. Y., "Theory of Steady State and Multiple Cracking of Random Discontinuous Fiber Reinforced Brittle Matrix Composites," *Journal of Engineering Mechanics*, V. 118, No. 11, 1992, pp. 2246-2264.
22. Lin, Z.; Kanda, T.; and Li, V. C., "On Interface Property Characterization and Performance of Fiber-Reinforced Cementitious Composites," *Journal of Concrete Science and Engineering*, V. 1, 1999, pp. 173-184.
23. Li, V. C., "Post-Crack Scaling Relations for Fiber-Reinforced Cementitious Composites," *Journal of Materials in Civil Engineering*, V. 4, No. 1, 1992, pp. 41-57.

24. Kanda, T., and Li, V. C., "Multiple Cracking Sequence and Saturation in Fiber Reinforced Cementitious Composites," *Concrete Research and Technology*, V. 9, No. 2, 1998, pp. 19-33.
25. Wu, H. C., and Li, V. C., "Snubbing and Bundling Effects on Multiple Crack Spacing of Discontinuous Random Fiber-Reinforced Brittle Matrix Composites," *Journal of the American Ceramics Society*, V. 75, No. 12, 1992, pp. 3487-3489.
26. Aveston, J.; Cooper, G. A.; and Kelly, A., "Single and Multiple Fracture," *The Property of Fiber Composite*, IPC Science and Technology Press, Guildford, UK, 1971.
27. Li, V. C.; Wang, S.; and Wu, C., "Tensile Strain-Hardening Behavior of Polyvinyl Alcohol Engineered Cementitious Composite (PVA-ECC)," *ACI Materials Journal*, V. 98, No. 6, Nov.-Dec. 2001, pp. 483-492.
28. Li, V. C.; Wu, C.; Wang, S.; Ogawa, A.; and Saito, T., "Interface Tailoring for Strain-Hardening Polyvinyl Alcohol-Engineered Cementitious Composite (PVA-ECC)," *ACI Materials Journal*, V. 99, No. 5, Sept.-Oct. 2002, pp. 463-472.
29. Lepech, M., and Li, V. C., "Water Permeability of Cracked Cementitious Composites," *Proceeding of Eleventh International Conference on Fracture*, Turin, Italy, 2005.
30. Lepech, M., and Li, V. C., "Durability and Long Term Performance of Engineered Cementitious Composites," *Proceedings of International RILEM Workshop on HPRCC in Structural Applications*, Honolulu, HI, 2005.
31. Redon, C.; Li, V. C.; Wu, C.; Hoshiro, H.; Saito, T.; and Ogawa, A., "Measuring and Modifying Interface Properties of PVA Fibers in ECC Matrix," *Journal of Materials in Civil Engineering*, V. 13, No. 6, 2001, pp. 399-406.
32. Mindess, S.; Young, J. F.; and Darwin, D., *Concrete*, 2nd Edition, Prentice Hall, 2002, 644 pp.
33. Weimann, M. B., and Li, V. C., "Hygral Behavior of Engineered Cementitious Composites (ECC)," *International for Restoration of Buildings and Monuments*, V. 9, No. 5, 2003, pp. 513-534.
34. Yang, Y.; Lepech, M.; and Li, V. C., "Self-Healing of ECC Under Cyclic Wetting and Drying," *Proceedings of the International Workshop on Durability of Reinforced Concrete under Combined Mechanical and Climatic Loads*, Qingdao, China, 2005.
35. Horikoshi, T.; Ogawa, A.; Saito, T.; and Hoshiro, H., "Properties of Polyvinylalcohol Fiber as Reinforcing Materials for Cementitious Composites," *Proceedings of International RILEM Workshop on HPRCC in Structural Applications*, Honolulu, HI, 2005.
36. Chan, Y. W., "Fiber/Cement Bond Property Modification in Relation to Interfacial Microstructure," Department of Civil and Environmental Engineering, University of Michigan: Ann Arbor, MI, 1994.
37. Kayali, O., "Effect of High Volume Fly Ash on Mechanical Properties of Fiber Reinforced Concrete," *Materials and Structures*, V. 37, No. 269, 2004, pp. 318-327.
38. Wang, S., and Li, V. C. "Polyvinyl Alcohol Fiber Reinforced Engineered Cementitious Composites: Material Design and Performance," *Proceedings of International RILEM Workshop on HPRCC in Structural Applications*, Honolulu, HI, 2005.
39. Atis, C. D., "High-Volume Fly Ash Concrete with High Strength and Low Drying Shrinkage," *Journal of Materials in Civil Engineering*, V. 15, No. 2, 2004, pp. 153-156.
40. Maslehuddin, M.; Saricimen, H.; and Al-Mani, A., "Effect of Fly Ash Addition on the Corrosion Resisting Characteristics of Concrete," *ACI Materials Journal*, V. 84, No. 1, Jan.-Feb. 1987, pp. 42-50.
41. Bisailon, A.; Rivest, M.; and Malhotra, V. M., "Performance of High-Volume Fly Ash Concrete in Large Experimental Monoliths," *ACI Materials Journal*, V. 91, No. 2, Mar.-Apr. 1994, pp. 178-187.
42. Li, V. C.; Lepech, M.; Wang, S.; Weimann, M.; and Keoleian, G., "Development of Green ECC for Sustainable Infrastructure System," *International Workshop on Sustainable Development and Concrete Technology*, Beijing, China, 2004.
43. Keoleian, G. A.; Kendall, A.; Dettling, J. E.; Smith, V. M.; Chandler, R.; Lepech, M. D.; and Li, V. C., "Life Cycle Modeling of Concrete Bridge Design: Comparison of Engineered Cementitious Composite Link Slabs and Conventional Steel Expansion Joints," *Journal of Infrastructure Systems*, ASCE, V. 11, No. 1, 2005, pp. 51-60.